SEMARAK ILMU PUBLISHING

Semarak International Journal of Petroleum and Chemical

Journal homepage:
https://semarakilmu.my/index.php/sijpce/index
ISSN: 3083-9106

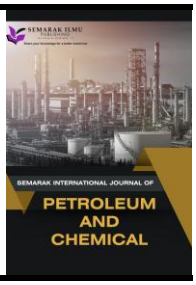

Optimizing Proton Exchange Membrane Fuel Cell across Varied Inlet and Outlet Dimensions

C.T Aisyah Sarjuni[1], Bee Huah Lim[1,*], Edy Herianto Mailan[1], Masli Irwan Rosli[1,2]

[1] Fuel Cell Institute, Universiti Kebangsaan Malaysia, Bangi, Malaysia
[2] Faculty of Engineering and Built Environment, Universiti Kebangsaan Malaysia, Bangi, Malaysia

ARTICLE INFO

Article history:
Received 27 March 2025
Received in revised form 25 April 2025
Accepted 22 May 2025
Available online 30 June 2025

Keywords:
Fuel cell; inlet width; computational fluid dynamics; current density

ABSTRACT

A proton exchange membrane fuel cell (PEMFC) is a promising hydrogen energy converter to curb climate change and energy security through its application. The stability of PEMFC performance is related to the reactant uniformity along the flow field of the bipolar plate. An uneven distribution of reactants and products diminishes the overall electrochemical performance by obstructing ion and electron transport over the membrane electrode assembly region. A parallel flow field was employed to study the impact of different cathode inlet/outlet widths on the current density distribution in a PEMFC. Namely simulations A and B for the inlet/outlet width of 8 millimeters and 28 millimeters on the cathode side. Results showed that simulation B generated an even flow with a less drastic change in velocity and an 8078 Pascal lower pressure drop than simulation B. This significantly prevented partial flooding when having a larger inlet/outlet width, enhancing the reactant O2 crossflow across the cathode active area interface. Hence, simulation A attained a 24 % lower average current and power density than simulation B. The improvement in PEMFC performance when using large inlet/outlet width highlights the significance of performance improvement considering the inlet/outlet dimension to obtain the optimum design for future commercialization.

1. Introduction

The increasing global energy demand has become increasingly concerning especially with the environmental consequences. In order to sustain energy supply for long-term, a multi-pathway strategy is progressively employed. Hydrogen power plays a pivotal role as one of the main energy sources within the planned global energy mix. Following the growth of this industry, PEMFC have been a pivotal alternative, especially for mobile and stationary systems. PEMFC's domination in the fuel cell market, especially in the Asian region, can be attributed to its high-power density and relatively more straightforward mechanism, which only needs humidified hydrogen and oxygen to produce power, water, and heat [1–4]. In the process of PEMFC maturity and commercialization,

* *Corresponding author.*
E-mail address: beehuah@ukm.edu.my

https://doi.org/10.37934/sijpce.3.1.1525

there are still several challenges to be tackled for long-term durability and cost that are economically feasible. The PEMFC is constructed with a membrane electrode assembly (MEA) consisting of a gas diffusion layer (GDL), catalyst layer (CL) and polymer electrolyte membrane (PEM), all of which are sandwiched in between two bipolar plates equipped with flow fields.

Optimization of the bipolar plates and gas flow channels is essential to ensure efficient heat and reactant transport throughout the MEA. This will then improve the MEA durability and PEMFC reliability in the long run. Attaining maximum reactant and heat distribution while maintaining efficient water management and optimum power loading remains a critical challenge in PEMFC design. Multiple studies have shown that operating parameters such as the cathode reactant flowrate can improve cell performance by reducing cell starvation region and improve water management. Hassani et al. researched the impact of air flowrate towards the degradation rate of a PEMFC [5]. It was found that higher air flow rate increased water removal which gradually improved the PEMFC performance, allowing more active sites for oxygen reduction reaction. This result aligns with studies from [6–8]. Chen *et al.,* [6] highlighted that as the gas starvation area reduced with increasing air flow rate, the cell power output becomes more stable. Similarly, Yang *et al.,* [7] showed enhanced gas diffusion rate with higher air flow rate. However, they stressed that a specific fuel cell design is limited to a certain flow rate. Exceeding this flowrate will only [8] cause fuel wastage as there will be insignificant improvement in cell performance. Nguyen *et al.,* also showed that the cathode reactant crossover through the PEM increases with higher flow rate. This raises the concentration of oxygen diffusing through the membrane towards the anode side. When operated in a multiple-cell stack, González *et al.,* [9] showed similar trend in performance increase with greater cathode flow rate especially at higher current densities. Like Yang *et al.,* [7] they highlighted that oversupply of cathode flow rate may cause membrane dehydration with the increased water removal. Another way to enhance the reactant transport in a PEMFC is by optimizing the inlet/outlet configurations. Changes to this parameter may alter the pressure and velocity created by the moving fluid mass, which is the basis of the two-phase fluid homogeneity required to prevent dehydration, flooding and performance loss. Several works have proven the effect of having multiple inlet/outlets in a single flow field [10–13]. The drainage capability and pressure drop are easily manipulated depending on the location and number of inlet/outlets.

These changes result in a higher reactant concentration at the CL- GDL interface due to the optimized humidity levels. For instance, Wang *et al.,* [11] proposed a combined serpentine and interdigitated flow field, which had three inlets and one outlet. A single serpentine flow field with one inlet/outlet showed improved water drainage while reducing up to 87% of pressure drop, leading to a 13% higher peak power density. Zhang *et al.,* [12] investigated the impact of having additional outlet in different locations within a parallel flow field. The additional outlet raised the oxygen concentration especially towards the outlet region. Water saturation was significantly reduced when the additional outlet was placed in the middle of the flow field. Nonetheless, these studies utilise the same inlet/outlet dimensions. The inlet/outlet dimensions also affect the mass transport throughout the flow field and eventually towards the MEA interfaces as well [14–18].

Results generally showed that a smaller inlet/outlet or channel dimensions promote higher forced convection on the reactant gases, as a smaller area promotes higher fluid velocity. This increases the mass transfer rate and under-land cross flow, raising the performance through a higher reaction rate. Smaller channels contribute to a higher pressure, which could lessen the net power density. Liu *et al.,* [15] implemented micro-distributors of three different widths in between the distribution zone and channel inlets of a parallel flow field. As the width of the micro-distributor inlet decreases, higher fluid velocity is generated, thus increasing water removal at the cathode GDL. Zhang *et al.,* [16] showed that smaller channel width increases the overall current density, but the

cell reaches the concentration loss phase faster than a wider channel width. Considering the fluid entrance and exit within different channel dimensions affect the mass transport, studies that consider the design of distribution zone within a flow field may reveal a different outcome. This is because fluid must be dispersed from the inlet/outlet towards the distribution zone before travelling through the flow channels; in contrast to conventional channels with direct access from inlet/outlet to the flow channels. The emergence of newer studies employing flow fields with distribution zones further emphasises the need to investigate the effects of inlet/outlet dimensions especially for flow fields with a distribution zone [19,20]. For example, Zhang *et al.,* [19] use a wider cathode inlet/outlet dimension than the anode side to cater for the heavier density of oxygen reactant gas.

Hence, this paper aims to fill the research gap by conducting a computational fluid dynamics (CFD) simulation for two single-stack PEMFCs with parallel flow fields. Both stacks differ only in terms of the cathode inlet/outlet dimensions, while the anode inlet/outlet dimensions remain the same. The performance of both stacks was compared through the fluid flow, mass transport and electrochemical characteristics via graphical and numerical data. This research will aid in the design engineering of flow field patterns for further optimisation of PEMFCs in future works. The results will also provide insight into the correlation between fluid flow rate and fuel cell design towards PEMFC performance.

2. Methods

2.1 Computational Domain

The three-dimensional (3-D) simulation study was conducted using the commercial software ANSYS Fluent R2 2022. To highlight the impact of inlet/outlet dimensions, a well-researched design like parallel flow field is used. The base model for the flow field was taken from a previous study [21], which was inspired by several research from [19,20]. In contrast to Zhang *et al.,* [19] this research considers the distribution zone as a reaction area together with the parallel channels. Figure 1 shows the computational domain of the single-cell PEMFC simulation models. Two configuration models with different cathode inlet/outlet dimensions were employed. The inlet width for the cathode flow field in simulation A is 8 millimeters, whereas in simulation B is 28 millimeters. For the anode side, a single inlet/outlet width of 8 millimeters is used for both simulations. The total active area is 27 square centimeters with a channel and rib cross-sectional area of 1 square millimeter. All anode and cathode flow fields are identical with 17 channels each.

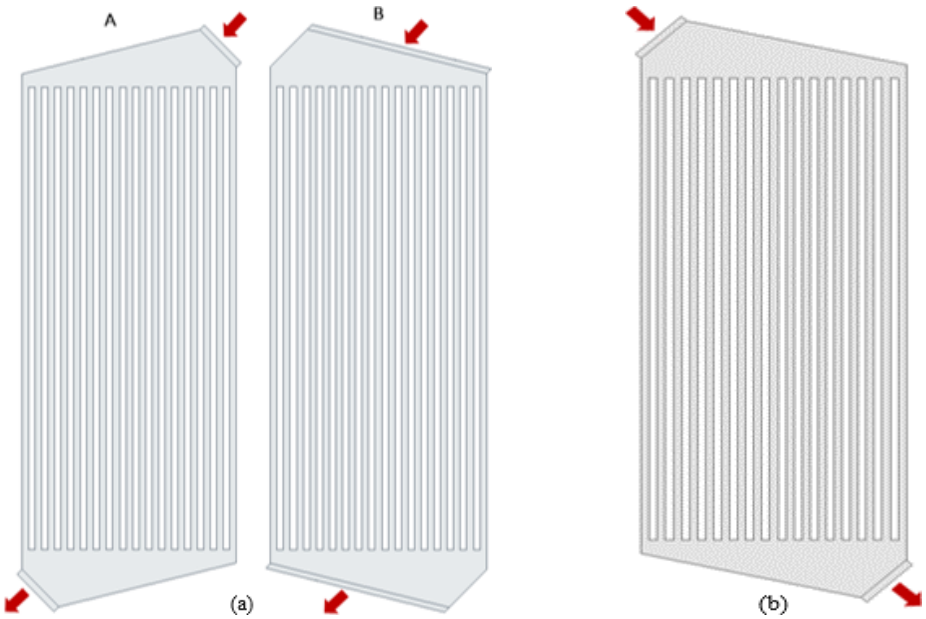

Fig. 1. Flow field used for simulation A and B of (a) cathode side, (b) anode side

The construction of model geometry is followed by defining the boundary conditions for each model domain to prepare for the computational fluid dynamics (CFD) simulation. The model parameters are defined in Table 1. The simulation model was solved using the Semi-Implicit Method for Pressure-linked Linked Equations (SIMPLE) algorithm for velocity-pressure coupling with convergence criteria of 10-6 for all residuals. The overall Fluent setup was carried out based on the assumptions listed below:

i. Two-phase flow model with laminar flow.
ii. Steady-state reaction.
iii. Gravity effect is neglected.
iv. All porous media are isotropic materials.

Table 1
Model Parameters

Parameter	Value
Temperature (K)	343
Pressure (atm)	1
Operating Voltage (V)	0.6
Anode Stoichiometric Ratio	5
Cathode Stoichiometric Ratio	10
GDL Thickness (µm)	35
CL Thickness (µm)	1
PEM Thickness (µm)	5

2.2 Governing Equations

Based on the assumption above, the governing equations to model this simulation research can be simplified according to the equations below:

Mass conservation equation:

$$\nabla.(\varepsilon\rho\vec{u}) = S_m \quad (1)$$

Where ε is porosity, ρ is the density, $\vec{u}$ is the fluid velocity and S_m is the quality source term.

Momentum conservation equation:

$$\frac{1}{\varepsilon^2}\nabla.(\rho\vec{u}\mu) = -\nabla p + \frac{1}{\varepsilon}\nabla\cdot(\mu\nabla\vec{u}) + S_u \quad (2)$$

Where p is pressure and μ is the fluid viscosity. S_u is the momentum source term which describes the physical characteristics of a porous media. This source term is also related to permeability in the equation:

$$S_u = -\mu_{eff}\varepsilon^2 u/_k \quad (3)$$

Energy equation:

$$\nabla\cdot\left(\rho C_p\varepsilon\vec{u}T = \nabla\cdot(k^{eff}\nabla T) + S_T\right) \quad (4)$$

where T, C_p and S_T represents temperature, specific heat capacity and energy source term respectively. Meanwhile, k^{eff} is the effective thermal conductivity which can be expressed further in equation (5), noting that k^f and k^s are the thermal conductivity of fluid and solid respectively.

$$k^{eff} = \varepsilon k^f + (1-\varepsilon)k^s \quad (5)$$

2.2 Grid Independence Test & Model Validation

A grid independence test (GIT) ensures that the simulation run is independent of the mesh size with maximum result accuracy. It is also critical to identify the optimum mesh size for time-efficient simulation. The test was done using the design of simulation A at three different mesh sizes, where the number of divisions was increased from 4, 6, and 8 at the channel, CL and PEM layers. Figure 2 shows that employing layer division of 6 is sufficient for the model to generate minimal error of 0.35%. As for model validation, the result from simulation B is compared with the reference study by Zhang *et al.,* [16] which was operated at similar operating conditions and flow field dimensions [20]. It was found that the current density at 0.65V differs by 5%, thus validating the accuracy of the simulation model.

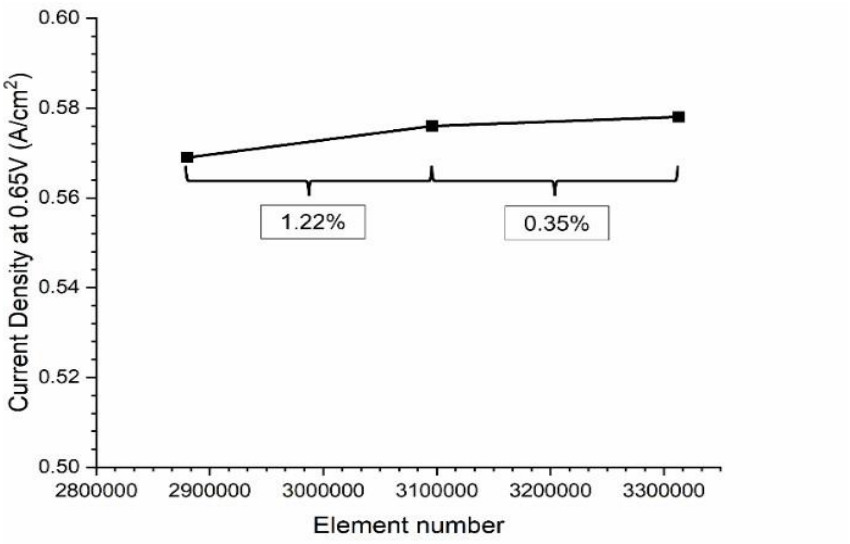

Fig. 2. Current density generation with different element number for grid independence test at 0.65V

3. Results

The simulated data were assessed through the simulation contours and numerical values taken at the appropriate interfaces according to the parameter assessed. The effects of varying cathode inlet dimensions and maintaining the anode inlet dimension at the same flow rate toward cell performance were observed and discussed below.

Figure 3 shows the velocity magnitude of simulations A and B in between the interface of the channel and GDL. The fluid velocity range in Figure 3(a) of the anode flow field in both simulations was similar at below 0.5 meters per second, due to the same inlet/outlet area. In contrast, the difference in fluid flow rate shown in Figure 3(b) was drastically different for the cathode side, where simulation A produced 86% higher peak fluid velocity than simulation B. There is a 50% decrease in cathode fluid velocity from 38 meters per second to 19 meters per second for simulation A. As a result, the cathode pressure drop reached 8773 pascal and 695 pascals for simulations A and B, respectively. This can be easily justified through Bernoulli's principle, where a change in velocity has an inverse effect on pressure [22]. Therefore, the higher velocity gradient acquired by simulation A generated a more considerable pressure drop than simulation B. Kinetic energy increases because of the higher fluid velocity, thus causing pressure to drop to balance the energy change for mass conservation. Moreover, a streamline of high-velocity fluid was formed through the smaller inlet area and was forced to disperse through the multiple-channel inlets. Instead of dispersing evenly, a dead-end area was produced in the last channel due to the minimal presence of fluid flow. The impact of this phenomenon can be discussed further by relating them with the reactant molar concentrations and resulting electrochemical output.

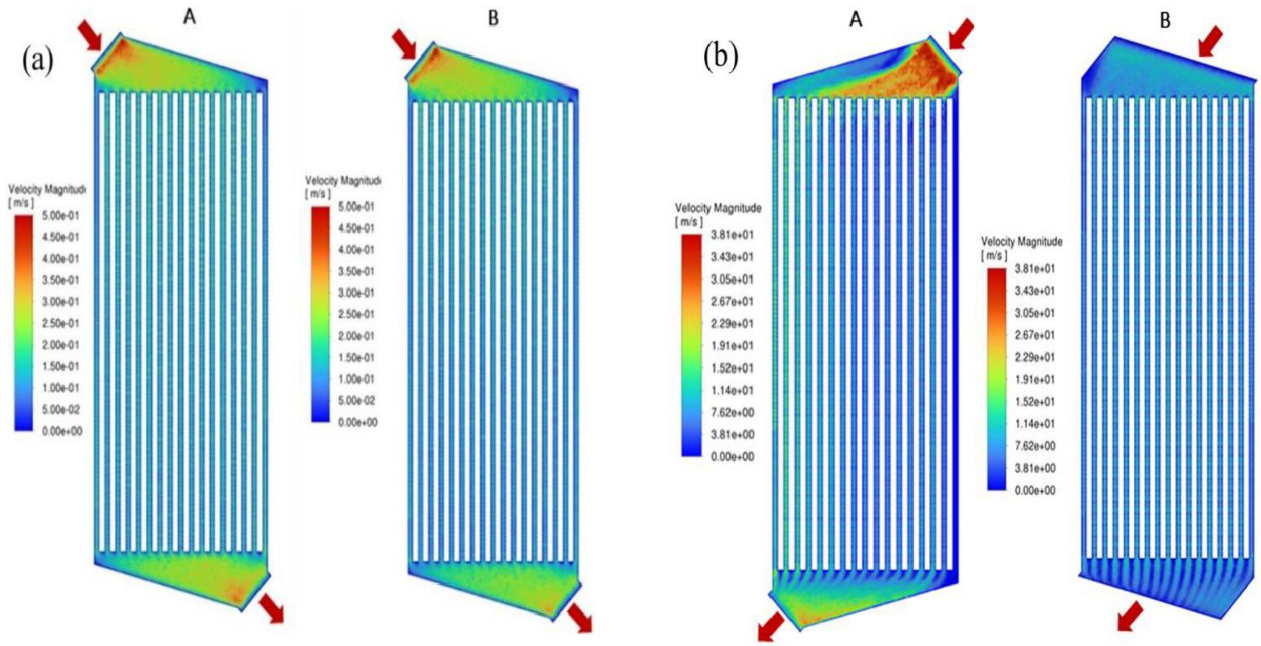

Fig. 3. Velocity distribution contour of simulation A and B at the channel-GDL layer (a) cathode side, (b) anode side

Since both simulations' anode inlet/outlet had the same dimensions, the hydrogen reactant and water product in Fig. 4 (a) and (b) had similar distribution patterns. The hydrogen consumption was noticeably faster in simulation B compared to simulation A, resulting in more water concentration in the channels of simulation B. Similar results were recorded at the cathode side in Fig. 5, whereby simulation B showed greater oxygen consumption than simulation A in Fig. 5(a). The minimal change in concentration gradient may indicate an oversupply of oxygen reactant at the cathode side, particularly in simulation A. Since the oxygen concentration is lower in simulation B, the high entrance velocity initiated by the smaller inlet width of simulation A could contribute to the excessive reactant surplus. The slower fluid velocity in simulation B allowed more oxygen flow control. Thus, the uniform fluid flow generated an even dispersion of oxygen reactant throughout the flow field. Meanwhile, partial flooding occurred in the last channel of simulation A, which is the same dead-end region seen in Fig. 5(b). The accumulation of excess water is detrimental to the performance of PEMFC as the water molecules may reduce the MEA layers' porosity, decreasing the permeability of reactants. The reduction in the available active surface area for reactant dissociation at the CL diminishes the overall cell performance due to concentration loss [23–25].

This is proven through the lower current density distribution recorded by simulation A in comparison to simulation B as seen in Fig. 6. This occurrence proves the impact of exceeding flow rate limitation for a specific PEMFC design [5–9]. The nature of design A may require a lower air stoichiometric ratio for optimised performance. The resulting power density at 0.6 volts came around to 0.34 watts per square centimeter and 0.44 watts per square centimeter for simulations A and B respectively. Moreover, the high-pressure drop generated by simulation A contributes to parasitic power, further reducing the net power output.

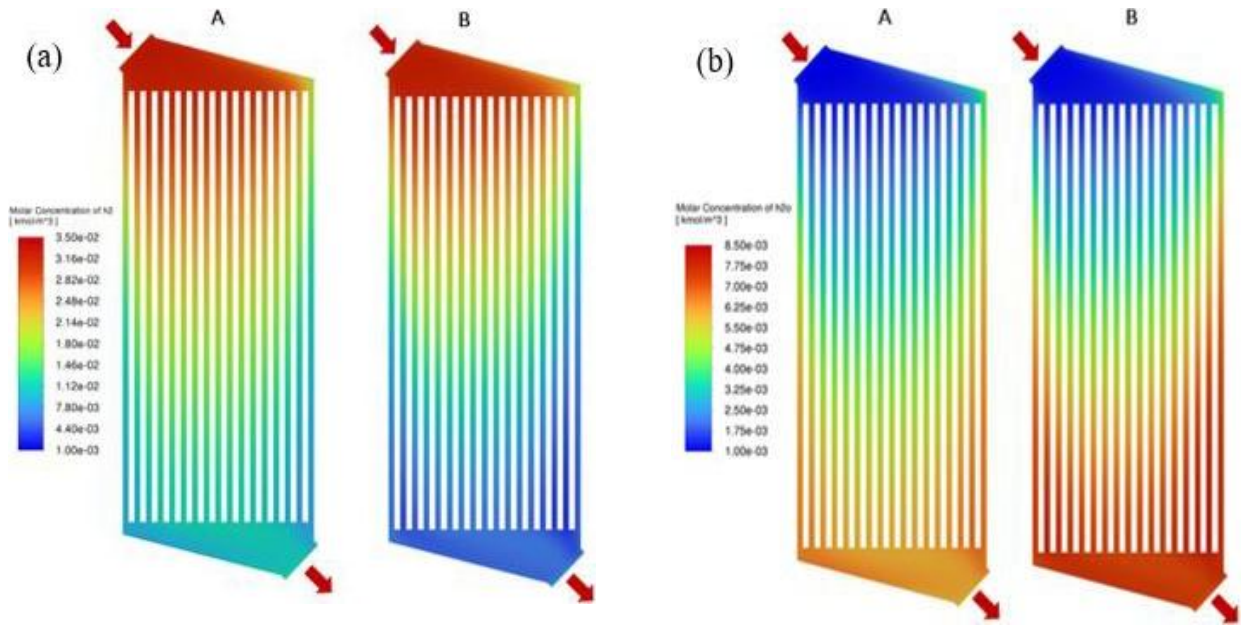

Fig. 4. Molar concentration at the channel-GDL interface for anode of simulation A and B (a) Hydrogen, (b) Water

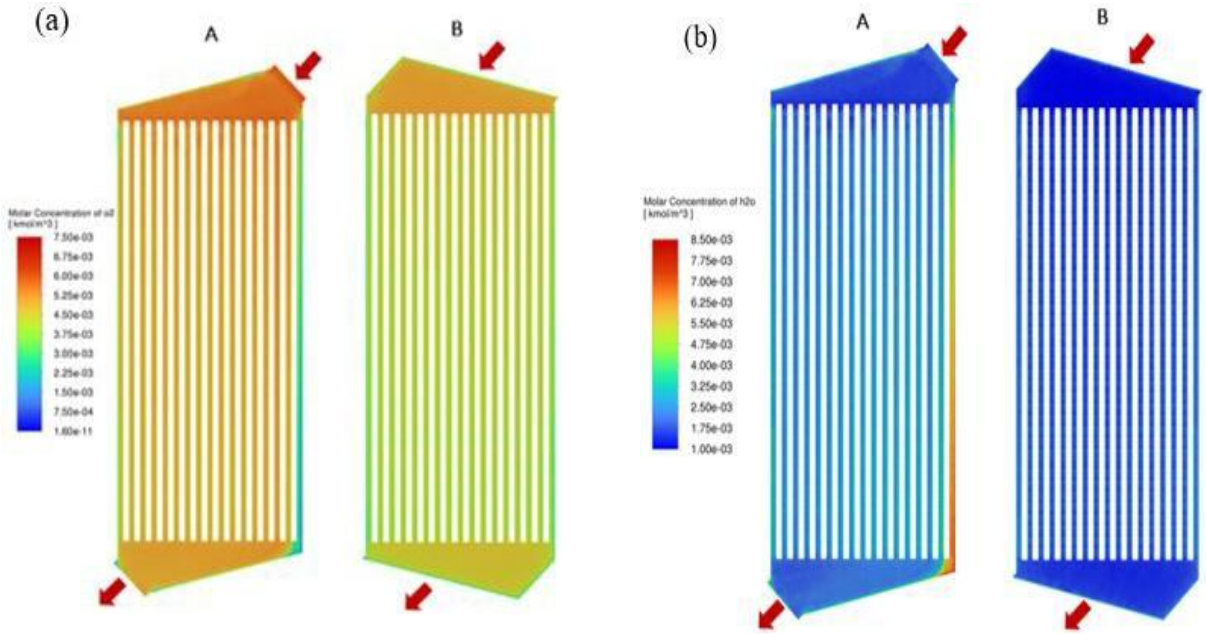

Fig. 5. Molar concentration at the channel-GDL interface for cathode of simulation A and B (a) Oxygen, (b) Water

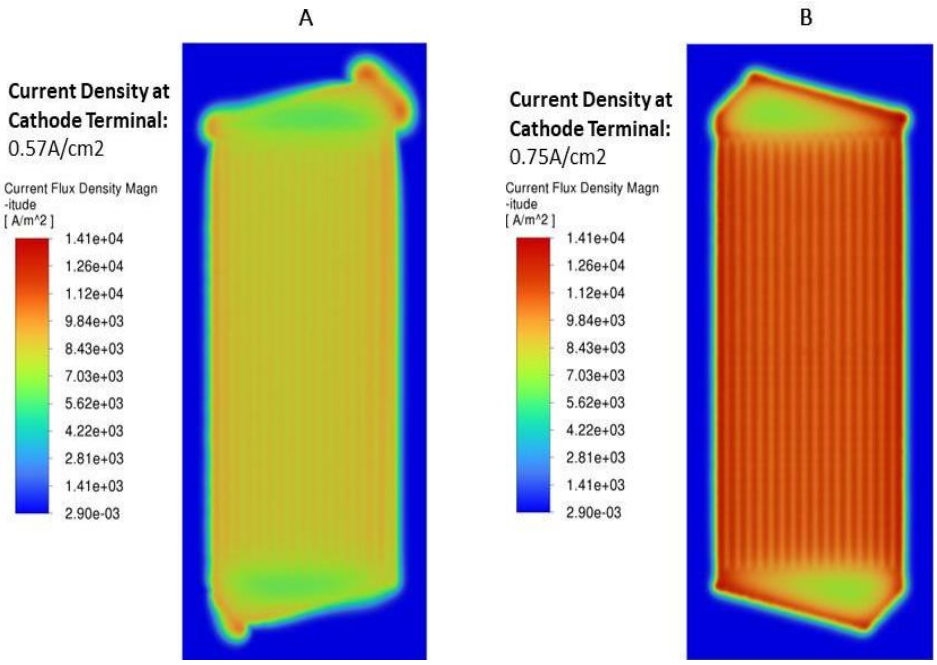

Fig. 6. Current distribution contour of simulations A and B at the CL-PEM interface

The industrial operation of PEMFC often calls for multiple cell stacks to achieve higher power generation. The mass transport of reactants is much more complicated due to the more significant number of layers that reactants must diffuse. Thus, the effect of partial flooding and lower current density generated by simulation A may be more apparent when constructed in a stack [26]. Therefore, the simulation results showed that employing an optimal flow field design is crucial as it can manipulate the fluid flow characteristics. It also proved the importance of considering the inlet/outlet dimension when designing a flow field, especially when used with higher flow rate. Uneven and uncontrolled fluid flow may trigger adverse effects such as flooding or dehydration that can diminish the electrochemical properties of the MEA layers.

4. Conclusion

This paper investigated the performance of two single-cell PEMFC with different inlet widths under the same operating conditions. Results show that although the anode side of simulations A and B had similar fluid velocity ranges, the resulting pressure difference generated varying hydrogen and water concentrations at the channel-GDL interface. Hydrogen reactant was consumed faster in simulation B than in simulation A, which naturally caused the excess water vapor to fill the consumed spaces downwards the channel. Water condensation can be mitigated by increasing the hydrogen supply rate to raise its dispersion area throughout the anode flow field. Meanwhile, simulation A on the cathode side exhibited poorer fluid flow homogeneity compared to simulation B, which formed partial flooding at the last channel. The higher water concentration in Simulation A ultimately led to a 24 percent lower average current and power density than in simulation B. The high-pressure drop generated by simulation A will also reduce the net power output, further reducing cell efficiency. In conclusion, the study showed the importance of considering the inlet/outlet conditions to acquire an optimum flow field simulation to maximize the active contact surface area and mass transport efficiency. Its effect will be much more evident in multiple-stacked PEMFCs, which will be an exciting research prospect on the impact of inlet/outlet dimensions.

Acknowledgement

The authors gratefully acknowledge the Higher Institution Centre of Excellent (HICoE) HICOE-2023-005 and Fundamental Research Grant Scheme, FRGS/1/2021/TK0/UKM/02/27 by the Ministry of Higher Education (MOHE), Malaysia in support of this work.

References

[1] Xu, Xiaofeng, Zhifei Wei, Qiang Ji, Chenglong Wang, and Guowei Gao. "Global renewable energy development: Influencing factors, trend predictions and countermeasures." *Resources Policy* 63 (2019): 101470. https://doi.org/10.1016/j.resourpol.2019.101470

[2] Yue, Meiling, Hugo Lambert, Elodie Pahon, Robin Roche, Samir Jemei, and Daniel Hissel. "Hydrogen energy systems: A critical review of technologies, applications, trends and challenges." *Renewable and Sustainable Energy Reviews* 146 (2021): 111180. https://doi.org/10.1016/j.rser.2021.111180

[3] Qussay, R., M. Mahmood, M. K. Al-Zaidi, R. Q. Al-Khafaji, D. K. Al-Zubaidy, and M. M. Salman. "A Review: Fuel Cells Types and their Applications." *Int. J. Sci. Eng. Appl. Sci* 7 (2021): 2395-3470.

[4] Zakaria, Zulfirdaus, Siti Kartom Kamarudin, and Khairul Anuar Abd Wahid. "Fuel cells as an advanced alternative energy source for the residential sector applications in Malaysia." *International Journal of Energy Research* 45, no. 4 (2021): 5032-5057. https://doi.org/10.1002/er.6252

[5] Hassani, M., Rahgoshay, S. M., Rahimi-Esbo, M., Dadashi Firouzjaei, K. "Experimental Study of Oxidant Effect on Lifetime of PEM Fuel Cell." *Iranian Journal of Hydrogen & Fuel Cell* 1 (2020): 33–43.

[6] Chen, Huicui, Liu, Biao, Liu, Runtian, Weng, Qianyao, Zhang, Tong, Pei, Pucheng. "Optimal interval of air stoichiometry under different operating parameters and electrical load conditions of proton exchange membrane fuel cell." *Energy Conversion and Management* 205 (2020): 112398. https://doi.org/10.1016/j.enconman.2019.112398

[7] Yang, Tien-Fu, Sheu, Bor-Hung, Mohammad, Ghalambaz, Yan, Wei-Mon. "Effects of operating parameters and load mode on dynamic cell performance of proton exchange membrane fuel cell." *International Journal of Energy Research* 45 (2020): 2474–2487. https://doi.org/10.1002/er.5942

[8] Nguyen, The-Truc, Fushinobu, Kazuyoshi. "Effect of operating conditions and geometric structure on the gas crossover in PEM fuel cell." *Sustainable Energy Technologies and Assessments* 37 (2020): 100584. https://doi.org/10.1016/j.seta.2019.100584

[9] González, M. Cabello, Toharias, Baltasar, Iranzo, Alfredo, Suárez, Christian. "Voltage distribution analysis and non-uniformity assessment in a 100 cm^2 PEM fuel cell stack." *Energy* 282 (2023): 128781. https://doi.org/10.1016/j.energy.2023.128781

[10] Sainan, Khairul Imran, Alhassan Salami Tijani, Irnie Azlin Zakaria, and Wan Ahmad Najmi Wan Mohamed. "Study of Multiple 2: 1 and Single 1: 1 inlet/outlet ratio for serpentine PEMFC performance." *Journal of Mechanical Engineering (JMechE)* 6 (2018): 1-9.

[11] Wang, Yixiang, Lei Wang, Xianhang Ji, Yulu Zhou, and Mingge Wu. "Experimental and numerical study of proton exchange membrane fuel cells with a novel compound flow field." *ACS omega* 6, no. 34 (2021): 21892-21899. https://doi.org/10.1021/acsomega.1c01924

[12] Zhang, Yan, Chenpeng Liu, Zhongmin Wan, Chen Yang, Shi Li, Zhengkai Tu, Min Wu, Yongqing Chen, and Wanchun Zhou. "Performance Enhancement of PEM Fuel Cells with an Additional Outlet in the Parallel Flow Field." *Processes* 9, no. 11 (2021): 2061. https://doi.org/10.3390/pr9112061

[13] Rosli, Masli Irwan, Bee Huah Lim, Edy Herianto Majlan, Teuku Husaini, Wan Ramli Wan Daud, and Soh Fong Lim. "Performance analysis of PEMFC with single-channel and multi-channels on the impact of the geometrical model." *Energies* 15, no. 21 (2022): 7960. https://doi.org/10.3390/en15217960

[14] Chowdhury, Mohammad Ziauddin, Omer Genc, and Serkan Toros. "Numerical optimization of channel to land width ratio for PEM fuel cell." *International Journal of Hydrogen Energy*43, no. 23 (2018): 10798-10809. https://doi.org/10.1016/j.ijhydene.2017.12.149

[15] Liu, Haichao, Weimin Yang, Jing Tan, Ying An, and Lisheng Cheng. "Numerical analysis of parallel flow fields improved by micro-distributor in proton exchange membrane fuel cells." *Energy Conversion and Management* 176 (2018): 99-109. https://doi.org/10.1016/j.enconman.2018.09.024

[16] Zhang, Xuyang, Andrew Higier, Xu Zhang, and Hongtan Liu. "Experimental studies of effect of land width in PEM fuel cells with serpentine flow field and carbon cloth." *Energies* 12, no. 3 (2019): 471. https://doi.org/10.3390/en12030471

[17] Badduri, Srinivasa Reddy, and Ramesh Siripuram. "Effect of Width of a Serpentine Flow Channel on PEM Fuel Cell Performance." *Proceedings of the Recent Advances in Renewable Energy Sources-RARES2021* (2021). https://doi.org/10.2139/ssrn.3822344

[18] Hassan, Gundu Mohamed, Jaeseung Lee, C. Muhammad Faizan, and Hyunchul Ju. "Numerical Study on the Cathode Channel Width Ratio for Improving Performance of Air Cooled PEMFC." In *2019 10th International Renewable Energy Congress (IREC)*, pp. 1-5. IEEE, 2019. https://doi.org/10.1109/IREC.2019.8754562

[19] Zhang, Yong, He, Shirong, Jiang, Xiaohui, Ye, Yuntao, Xiong, Mu, Yang, Xi. "Characteristics of proton exchange membrane fuel cell considering "dot matrix" gas distribution zones and waveform staggered flow field with cooling channels." *Energy Conversion and Management*, 267 (2022): https://doi.org/10.1016/j.enconman.2022.115881

[20] Zhang, Yong, He, Shirong, Jiang, Xiaohui, Xiong, Mu, Ye, Yuntao, Yang, Xi. "3D multi-phase simulation of metal bipolar plate proton exchange membrane fuel cell stack with cooling flow field." *Energy Conversion and Management* 273 (2022): https://doi.org/10.1016/j.enconman.2022.116419

[21] Sarjuni, CT Aisyah, Bee Huah Lim, Edy Herianto Majlan, Masli Irwan Rosli, and Wai Yin Wong. "Analysis of fluid flow behaviour in different proton exchange membrane fuel cell flow field configurations." *Asia-Pacific Journal of Chemical Engineering* 18, no. 6 (2023): e2939. https://doi.org/10.1002/apj.2939[22]

[22] Saleta, Martın Eduardo, Dina Tobia, and Salvador Gil. "Experimental study of Bernoulli's equation with losses." *American journal of physics* 73, no. 7 (2005): 598-602. https://doi.org/10.1119/1.1858486

[23] Shen, Jun, Liang Xu, Huawei Chang, Zhengkai Tu, and Siew Hwa Chan. "Partial flooding and its effect on the performance of a proton exchange membrane fuel cell." *Energy Conversion and Management* 207 (2020): 112537. https://doi.org/10.1016/j.enconman.2020.112537

[24] Daud, Wan RW, Elly D. Rahman, Putri A. Mulya, and Nia G. Sari. "EFFECT OF OPERATING CONDITIONS ON THE LIQUID WATER CONTENT FLOWING OUT OF THE CATHODE SIDE AND THE STABILITY OF PEM FUEL CELL PERFORMANCE." *International Journal of Technology* 10, no. 3 (2019). https://doi.org/10.14716/ijtech.v10i3.2929

[25] Liu, Xuan, Hang Guo, Fang Ye, and Chong Fang Ma. "Water flooding and pressure drop characteristics in flow channels of proton exchange membrane fuel cells." *Electrochimica Acta*52, no. 11 (2007): 3607-3614. https://doi.org/10.1016/j.electacta.2006.10.030

[26] Peng, Yimeng, Xiaohui Yan, Chen Lin, Shuiyun Shen, Jiewei Yin, and Junliang Zhang. "Effects of flow field on thermal management in proton exchange membrane fuel cell stacks: A numerical study." *International Journal of Energy Research* 45, no. 5 (2021): 7617-7630. https://doi.org/10.1002/er.6343